# CHAPTER II

# THEORY & LITERATURE REVIEWS

## 2.1 Gas chromatographic separation of enantiomers

Gas chromatography (GC) is usually considered as an accurate and reliable technique for the separation of volatile and thermally stable organic compounds. Its advantages include high efficiency, sensitivity, reproducibility, and speed of separation [6]. For chiral separation using GC, two approaches can be performed: direct and indirect approaches. The indirect approach involves derivatization of the chiral compounds with an auxiliary chiral reagent to convert enantiomers into diastereomers which then be separated by any achiral separation techniques. Many disadvantages of this approach include the requirement of purely chiral reagent, long analysis time (sample preparation and identification), inconvenience, and possible biased results for enantiomeric composition due to partial racemization during derivatization. Moreover, discrimination by incomplete recovery or loss due to decomposition may occur during work-up, isolation, and sample handling [7]. On the other hand, the direct approach involves the use of chiral stationary phase (CSP) as a selector which directly form transient diastereomeric intermediates with the chiral analyte.

Among several chiral selectors, CDs and their derivatives are frequently used in GC because of their ability to form inclusion complexes with various types of substances. Moreover, the wide operating temperature of CDs and their derivatives makes them one of the most versatile stationary phases for GC [8,9].

## 2.2 Cyclodextrins and their derivatives

Cyclodextrins (CDs) are cyclic oligosaccharides produced from enzymatic degradation of the linear amylose component of starch by cyclodextrin glucanotransferases (CGTases). The three most common CDs compose of six, seven, and eight D-glucose units linked by α-1,4-glycosidic bond; referred to α-, β- and γ-

CDs, respectively [19]. Molecular dimension and some physical properties of the three native CDs are summarized in Table 2.1.

**Table 2.1** Molecular dimensions and physical properties of native CDs [19].

| | α-CD | β-CD | γ-CD |
|---|---|---|---|
| Number of glucopyranose units | 6 | 7 | 8 |
| Chemical formula | $(C_6H_{10}O_5)_6$ | $(C_6H_{10}O_5)_7$ | $(C_6H_{10}O_5)_8$ |
| Number of chiral centers | 30 | 35 | 40 |
| Anhydrous molecular weight (g/mol) | 972.85 | 1134.99 | 1297.14 |
| Internal diameter (Å) | 4.7–5.3 | 6.0–6.5 | 7.5–8.3 |
| Cavity depth (Å) | 7.9 | 7.9 | 7.9 |
| Cavity volume ($Å^3$) | 174 | 262 | 427 |
| Water solubility (g/100 mL, 25 °C) | 14.50 | 1.85 | 23.20 |
| Decomposition temperature (°C) | 278 | 299 | 267 |

Native CDs are frequently characterized as a doughnut or wreath-shaped truncated cone. In each glucopyranose unit of CD contains secondary hydroxyl groups at C2 and C3 positions on the wide rim and the primary hydroxyl groups at C6 position on the narrow edge (Figure 2.1). The two perimeters of the CD molecule are hydrophilic while the interior surface is hydrophobic. CDs (as host molecules) can form inclusion complexes with a wide variety of analyte molecules (as guest molecules) [8,9,19].

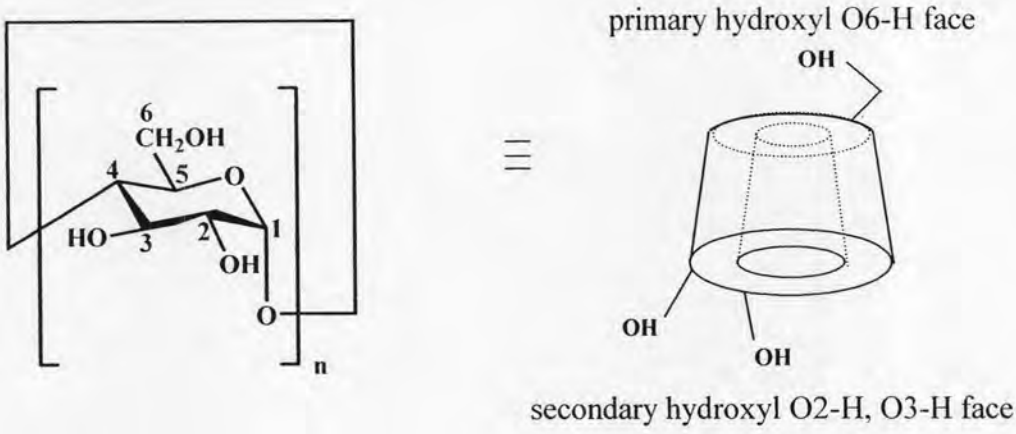


**Figure 2.1** Structure of CD molecule with n glucose units (left) resembling a truncated cone (right) with primary hydroxyl O6-H groups on the narrower side and secondary hydroxyl O2-H, O3-H groups on the wider side.

## 2.3 Gas chromatographic separation of enantiomers using cyclodextrin derivatives

Natural CDs have been proven to be unfavorable for using as stationary phases in capillary GC because they are solid at room temperature, have limited operating temperature range, and have low solubility in polysiloxane diluent. Therefore, they are unsuitable for coating the capillary columns and give the coated columns with very low efficiency. However, natural CDs can be chemically modified to improve their physical and chemical properties, such as decomposition temperature and solubility, by substituting various functional groups at the primary and/or secondary hydroxyl groups. In general, the secondary hydroxyl groups at C2 and C3 positions of each glucose unit are modified with small alkyl or acyl groups to change the enantioselectivity, whereas the primary C6 hydroxyl groups are replaced with longer alkyl or bulky groups to change polarity, viscosity, or solubility in polysiloxane [6,7].

As described above, the enantiomeric separation occurs by generating a transient diastereomeric intermediate between the chiral analyte and CSP. The chiral recognition process involves various forces between the chiral analyte and CSP such as dispersion force, dipole-dipole interaction, and hydrogen bonding [6–9]. Derivatization of the free CD hydroxyls changes the type of interactions between the

analyte and CSP. Thus, the chiral discriminations are generally different for each enantiomeric pair.

Previous researches have been demonstrated that enantioseparation by GC using CD derivatives as chiral selectors is governed by the size and shape of CDs, the concentration of CDs in polysiloxane, the separation temperature, and the structure of chiral analytes [11−17, 20−27]. Important results obtained from previous studies can be summarized as follows:

McGachy and co-workers [11] used permethylated β-CD (Me-CD) as a chiral selector to study the separation of 12 pairs of *N*-trifluoroacetyl-*O*-alkylnipecotic acid ester enantiomers. The results show that the *n*-alkyl esters interact with Me-CD stronger than do the esters containing α-branched alkyl groups although the latter exhibits higher enantioselectivity than does the former.

Skórka and co-workers [12] investigated the influence of both the size of CDs and structure of monoterpenoids on enantiodifferentiation. The results indicate that α-CD better accommodates the monoterpenoids than does on β-CD. The thermodynamic data (e.g. enthalpy, entropy, and free energy) are higher for bicyclic than for monocyclic monoterpenoids for both α-CD and β-CD.

Nie and co-workers [20] separated the enantiomers of amines, alcohols, diols carboxylic acids, amine acids, epoxides, halohydrocarbons, and ketones by GC using three derivatized β-CDs as CSPs: heptakis-(2,6-di-*O*-nonyl-3-*O*-trifluoroacetyl)-β-CD (DNTBCD); heptakis-(2,6-di-*O*-dodecyl-3-*O*-trifluoroacetyl)-β-CD (DDTBCD); and heptakis-(2,6-di-*O*-pentyl-3-*O*-trifluoroacetyl)-β-CD (DPTBCD). The results show that DNTBCD exhibits the best chiral selectivity among the three stationary phases. In addition, thermodynamic data of chiral separation of α-phenylethylamine derivatives indicate that the separation using both DNTBCD and DPTBCD are directed by the same chiral recognition mechanism.

Anderson and co-workers [21] separated the 17 chiral sulfoxides and 8 chiral sulfinate esters by GC using four types of CD derivatives: 2,6-di-*O*-pentyl-3-

trifluoroacetyl-γ-CD (G-TA); 2,6-di-*O*-pentyl-3-propionyl-γ-CD (G-PN); 2,6-di-*O*-pentyl-3-butyryl-γ-CD (G-BP); and 2,6-di-*O*-methyl-β-CD (B-DM). The results indicate that G-PN and G-BP exhibit similar selectivity and resolution for most of the analytes. Among the three γ-CD derivatives mentioned above, G-TA exhibits superior enantioselectivity for most sulfoxides and sulfinate esters. However, B-DM providing the best enantioselectivity for most of sulfinate esters. The size and polarity of sulfoxide substituents affect their enantioselectivities on all CSPs. Moreover, G-TA and B-DM provide opposite elution order of enantiomers is probably due to the differences in sizes and substituents of CDs.

Tisse and co-workers [22] separated the enantiomers of secondary alcohols, γ-lactones, hydantoin derivatives, and 1-phenylethanol derivatives using three derivatized β-CD stationary phases: $2^{I}$-*O*-methoxycarbonylmethyl-$2^{II-VII}$,$3^{I-VII}$,$6^{I-VII}$-eicosa-*O*-methyl-cyclodextrin (20Me/P2OCH2COOMe); $6^{I}$-*O*-methoxycarbonyl methyl-$2^{I-VII}$,$3^{I-VII}$,$6^{II-VII}$-eicosa-*O*-methyl-cyclodextrin (20Me/P6OCH2COOMe); and $6^{I}$-*O*-methoxycarbonyl-$6^{I}$-deoxy-$2^{I-VII}$,$3^{I-VII}$,$6^{II-VII}$-eicosa-*O*-methylcyclodextrin (20Me/P6COOMe). The results show that the four CSPs possess similar enantioseparation abilities for the analytes studied. However, for most cases, the 20Me/P2OCH2COOMe exhibits the best enantioselectivity than do the other selectors.

Shi and co-workers [23] examined the influence of substitution type and position on CD ring on the enantiomeric separation of alcohols, esters, and epoxides by GC using four derivatized-β-CDs as CSPs: 2,6-di-*O*-pentyl-3-*O*-allyl-β-CD; 2,3-di-*O*-pentyl-6-*O*-allyl-β-CD; 2,6-di-*O*-pentyl-3-*O*-propyl-β-CD; and 2,3-di-*O*-pentyl-6-*O*-propyl-β-CD. The results indicate that the four CSPs possess similar enantioseparation abilities towards allethrone acetate, propargyllone, 2-bromopropionic acid methyl ester, 2-chloropropionic acid methyl ester, and some enantiomers of epoxides. However, all CSPs show no enantioseparation abilities towards all pyrethroic acid methyl esters and 5-hydroxy-4,4-dimethyl-dihydrofuran-2-one.

Shi and co-workers [24] also separated the enantiomers of 7 chiral epoxides by GC using four derivatized β-CDs: 2,6-di-*O*-benzyl-3-*O*-heptanonyl-β-CD (column 1);

2,6-di-*O*-benzyl-3-*O*-octanonyl-β-CD (column 2); 2,3-di-*O*-benzyl-6-*O*-heptanonyl-β-CD (column 3); and 2,3-di-*O*-benzyl-6-*O*-octanonyl-β-CD (column 4). The results suggest that column 1 is more favorable for enantioseparation of the epoxides than column 2. Therefore, heptanonyl substituted on 3-position of CD is more favorable for enantioseparation of the epoxides than octanonyl substituted on the same position. While columns 3 and 4 possess similar enantioseparation abilities to the epoxides. These results indicate that both the substitution type and position on CD ring have great influence on the enantioselectivities of epoxides.

The 6-*O*-tert-butyldimethylsilyl derivatives of CDs have been proven to be valuable chiral selectors and are widely used for enantiomer separation by GC. The enantioselectivities as well as some selected applications of these CSPs are summarized as follows:

Kobor and Schomburg [25] studied the influence of CD ring size on the enantioseparation of homologous series of 1-phenylalkanols using 6-*tert*-butyl dimethylsilyl-2,3-dimethyl derivatives of α-, β-, and γ-CDs (TB-α-CD, TB-β-CD, and TB-γ-CD, respectively) as CSPs. The results indicate that 1-phenylalkanols with short side chains, such as 1-phenylethanol and 1-phenyl-1-propanol, exhibit greater enantioselectivity on TB-α-CD, whereas the larger ring β-CD derivative is more enantioselective for the analytes with longer side chain lengths such as 1-phenyl-1-butanol and 1-phenyl-1-pentanol. Nonetheless, no enantiomeric separation of any homologous 1-phenylalkanols could be resolved on the TB-γ-CD derivative.

Vetter and co-workers [26] studied the enantioseparation of the 26 chiral organochlorine compounds using heptakis(6-*O*-*tert*.-butyldimethylsilyl-2,3-di-*O*-methyl)-β-CD (β-TBDM) as CSPs. One CSP was made of pure β-TBDM while the others were made of the randomly silylated β-TBDM. The randomly silylated β-TBDM resolved the enantiomers of 24 compounds (16 of them were baseline separated), whereas the pure β-TBDM resolved only 6 compounds (4 of them were baseline separated). The results demonstrate that the randomly silylated β-TBDM is more suitable for the enantioseparation of organochlorine compounds than the pure β-TBDM.

Takahisa and Engel [27] separated the enantiomers of various flavor compounds from different chemical classes using octakis(2,3-di-*O*-methoxymethyl-6-*O*-*tert*-butyldimethylsilyl)-γ-CD (2,3-MOM-6-TBDMS-γ-CD ) as chiral selector. The results show that 2,3-MOM-6-TBDMS-γ-CD is a versatile CSP for enantioseparation of a very broad spectrum of chiral volatiles from various functional groups. However, this column could not separate tertiary alcohols and their esters, bicyclic compounds, and less volatile esters. In addition, the range of compounds for which enantiomers could be separated with 2,3-MOM-6-TBDMS-β-CD was more limited and the enantioseparation achieved was less pronounced when compared with 2,3-MOM-6-TBDMS-γ-CD. [28]

Shitangkoon and co-workers [13] studied the relationship between the enantioseparation and the analyte structures of 19 aromatic alcohol derivatives by GC using heptakis(2,3-di-*O*-methyl-6-*O*-*tert*-butyldimethylsilyl)-β-CD in OV-1701 as CSP. The results show that the substitution on the aromatic ring of the alcohol tends to promote enantiodifferentiation, whereas substitution on the side chain likely reduces enantiodifferentiation.

Iamsam-ang [14] separated the enantiomers of 1-phenylethanol derivatives using heptakis(2,3,6-tri-*O*-methyl)-β-CD and heptakis(2,3-di-*O*-methyl-6-*O*-*tert*-butyldimethylsilyl)-β-CD as chiral selectors. The enantioselectivities of alcohol derivatives on both CSPs were highly affected by the position of substituent on the aromatic ring rather than the type of substituent. Further studies were performed by Konghuirob using octakis(2,3-di-*O*-methyl-6-*O*-*tert*-butyldimethylsilyl)-γ-CD (GSiMe) as a CSP [15]. The results agree with those studied by Iamsam-ang but the enantiodifferentiation of alcohol derivatives on GSiMe are small. And the latest studies were carried out by Pothisamutyothin using hexakis(2,3-di-*O*-methyl-6-*O*-*tert*-butyldimethylsilyl)-α-CD (ASiMe) as a CSP [17]. It was found that ASiMe could separate some chiral alcohols which could not be resolved on BSiMe and GSiMe. This indicates that the size and the structure of CD derivatives are affected the separation of enantiomers. Furthermore, GSiMe column is not suitable for the enantioseparation of alcohols because only a few alcohols can be well resolved.

## 2.4 Thermodynamic investigation of enantiomeric separation by gas chromatography

Although the mechanism of chiral recognition in chromatographic method is not well understood, some mechanistic aspects can be derived from the thermodynamic investigation of the reliable experimental parameters. In general, it is accepted that the direct enantiomeric separation is based on the formation of transient diastereomic complexes between enantiomers and a chiral selector by intermolecular interactions. For the complex formation, temperature is an important factor influencing the retention factor, enantioselectivity, and resolution. The chemical equilibrium between individual enantiomer and CSP can be described by thermodynamic data using the Gibbs–Helmholtz equation [6, 10].

Due to the simplicity of the van't Hoff approach, it is used to determine the thermodynamic parameters from retention factor (k′) and separation factor (α) obtained at different temperatures on a single chiral column.

In van't Hoff approach, the difference in Gibbs free energy, ΔΔG, is calculated from the separation factor (α) obtained from enantiomeric separation on a chiral column at a given temperature according to equation (1):

$$-\Delta\Delta G = RT \cdot \ln \alpha = RT \cdot \ln\left(\frac{k_2'}{k_1'}\right) \quad \text{(cal/mol)} \quad (1)$$

where $\alpha$ is the separation factor or selectivity obtained from the ratio of k′ of two enantiomers

$k'$ is the retention factor or capacity factor of each enantiomer calculated from solute retention time according to

$$k' = \frac{t_R - t_M}{t_M}$$

$t_R$ is the retention time of an enantiomer or analyte

$t_M$ is the time for unretained compound to travel at the same distance as analyte

R is the universal gas constant (1.987 cal/mol·K)

$T$ is the absolute temperature (K)

1,2 refer to the less and the more retained enantiomers, respectively

Combining equation (1) with the Gibbs-Helmholtz relationship, equation (2), leads to equation (3):

$$-\Delta\Delta G = -\Delta\Delta H + T\cdot \Delta\Delta S \quad (2)$$

$$R T \cdot \ln\alpha = -\Delta\Delta H + T\cdot \Delta\Delta S \quad (3)$$

Equation (3) can be rewritten as

$$\ln \alpha = \frac{-\Delta\Delta H}{RT} + \frac{\Delta\Delta S}{R} \quad (4)$$

where $\Delta\Delta H$ is the difference in enthalpy for an enantiomeric pair

$\Delta\Delta S$ is the difference in entropy for an enantiomeric pair

According to equation (4), $\Delta\Delta H$ and $\Delta\Delta S$ could be evaluated from the slope and y-intercept of the ln $\alpha$ versus 1/T plot. However, the calculations of thermodynamic parameters from these plots are not possible, as a result of curvatures observed in many cases. This is due to the nonlinear dependence of selectivity on the concentration in diluted stationary phase. Therefore, this method is only valid for undiluted chiral selectors [10].

Alternatively, thermodynamic parameters can be calculated from retention factors (k′) instead of separation factors ($\alpha$). The linear relationship between ln k′ and 1/T can be derived from the combination of equations (5) and (6) resulted in equation (7). Thermodynamic parameters of individual enantiomers including the differences in enthalpy and entropy of an enantiomeric pair can be obtained from the plot of ln k′ against 1/T.

$$-\Delta G = RT \cdot \ln K = RT \cdot \ln (k'\cdot\beta) \quad (5)$$

$$-\Delta G = -\Delta H + T\cdot \Delta S \quad (6)$$

$$-\Delta H + T\cdot \Delta S = RT \cdot \ln(k'\cdot\beta)$$

$$\frac{-\Delta H}{RT} + \frac{\Delta S}{R} = \ln k' + \ln\beta$$

$$\ln k' = \frac{-\Delta H}{RT} + \frac{\Delta S}{R} - \ln\beta \quad (7)$$

where K is the distribution coefficient of chiral analyte between gas phase and liquid phase

β is a constant called phase ratio (the ratio of mobile phase volume to stationary phase volume)

ΔH is enthalpy change resulting from the interaction of the enantiomer with the stationary phase. ΔH value describes the degree of the interaction strength. The more negative ΔH value indicates stronger interaction between analyte and stationary phase.

ΔS is entropy change resulting from the interaction of the enantiomer with the stationary phase. ΔS describes the degree of which the solute structure influences the interaction.

## 2.5 Molecular modeling studies for enantioseparation

The chiral discriminations are governed by various factors, e.g. size, shape, and concentration of CD derivatives; type and position of substituents on CD rings; and analyte structure. However, the interactions between analytes and the CD derivatives that lead to enantiomer separations are not yet well understood. Therefore, molecular modeling calculations are performed for insight into the mechanism of chiral discrimination. Preceeding researches concerning the molecular modeling of CD-derivative in GC are summarized as follows.

Kobor and co-workers [29] performed theoretical calculations based on molecular docking to investigate the mechanism of chiral recognition of a nonpolar (limonene) and a polar (1-phenylethanol) compounds using permethyl-β-CD (PMCD) and 2,3-dimethyl-*tert*-butyldimethylsilyl-β-CD (TBCD) as chiral selectors. The results show that a more rigid CD cavity like TBCD exhibits higher enantioselectivity for nonpolar analyte than does the CD with a more flexible structure like PMCD.

Beier and Höltje [30] investigated the enantioselective binding properties of chiral dihydrofuranones on heptakis(2,3-di-*O*-methyl-6-*O*-*tert*-butyldimethylsilyl)-β-CD using annealed molecular dynamics simulation with program GRID. The

methodology for the construction of the interaction model gives the results in good agreement with the GC experimental data. The inclusion mechanism between the guest (dihydrofuranones) and the host (CD) is important for chiral recognition. The intermediate diastereomeric complex is stabilized by hydrogen bonds. The proposed induced-fit mechanism is also an essential contribution to the enantioselective binding between analyte and chiral selector. Nonetheless, the general applicability of the procedure described in this work has to be further proven.

Ramos and co-workers [31] separated the 2-alkyl-2-keto-γ-butyrolactone derivatives and their alcohol analogs using 2,3-di-*O*-methyl-6-*O*-*tert*-butyldimethyl silyl-β-CD (DIMETBCD) as a chiral selector. The results, supported by molecular modeling, suggest that the chiral recognition for DIMETBCD depended more on the geometry than on the polarity of the alkyl substituent on the butyrolactones. Furthermore, the hydrogen bonds and the alkyl group steric effects play an important role on chiral recognition.

## 2.6 Investigation of chiral recognition between CD and epoxide derivatives by molecular modeling

For the better understanding of the chiral recognition mechanism, several molecular modeling methods have been used, such as molecular dynamic simulation, molecular docking, etc. The molecular docking method has been widely used for some years. Its goal is to obtain the precise docking structure, which corresponds to the energetically most stable configuration. Furthermore, it provides simplicity and short calculation time.

In this work, the molecular docking and quantum mechanical calculations are applied to explain the chiral recognition between CD and epoxide derivatives (in the context of inclusion complexes, they are called "host" and "guest", respectively). Necessary background of molecular docking is given below.

### 2.6.1 Molecular Docking

The binding energy obtained from AutoDock 4.0.1 is derived from van der Waals potential and electrostatic potential terms [32].

***Van der Waals potential energy*** [32]

The pairwise potential energy, V(r), between two non-bonded atoms can be expressed as a function of internuclear separation, r, as follows:

$$V(r) = \frac{A}{r^{12}} - \frac{B}{r^{6}} \tag{8}$$

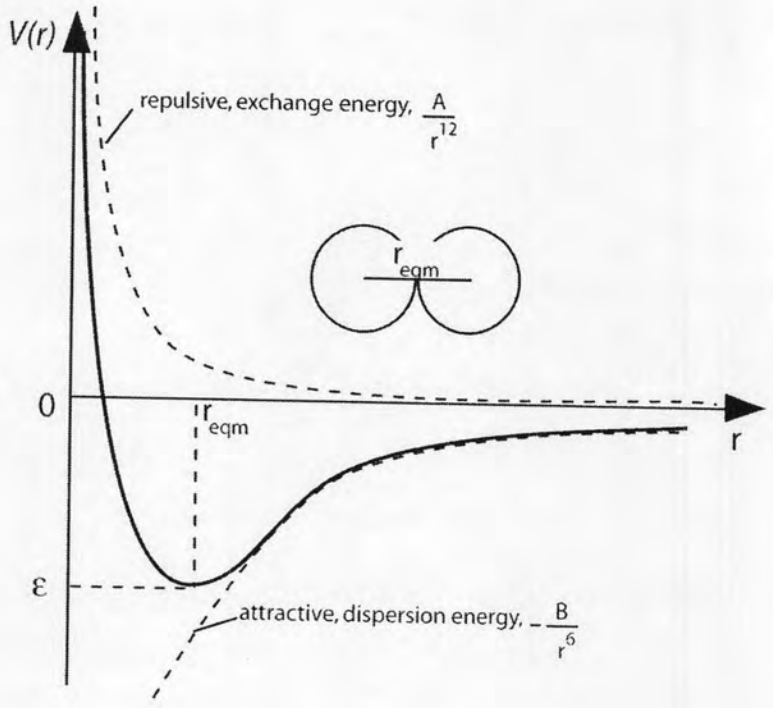


**Figure 2.2** Intermolecular pair potential energy curve.

Typically, the pair potential function with the 12-6 Lennard-Jones parameters are used to model the van der Waals forces experienced between two instantaneous dipoles as equation (9):

$$V(r) = \frac{C_{12}}{r^{12}} - \frac{C_{6}}{r^{6}} \tag{9}$$

However, the 12-10 form is used to model hydrogen bonding interactions according to equation (10):

$$V(r) = \frac{C_{12}}{r^{12}} - \frac{C_{10}}{r^{10}} \quad (10)$$

Therefore, pairwise-atomic interaction energies can be approximated using the following general equation:

$$V(r) = \frac{C_n}{r^n} - \frac{C_m}{r^m} = C_n r^{-n} - C_m r^{-m} \quad (11)$$

where m and n are integers.

$C_m$ and $C_n$ are constants whose values depend on the depth of the energy well and equilibrium separation of the two atoms nuclei.

A revised set of parameters has been calculated, which uses the same van der Waals radius of a given atom for all pairwise distances, no matter what the other atom. Likewise, the well-depths are consistently related. Let $r_{eqm,aa}$ be the equilibrium internuclear separation between the nuclei of two atoms a. A derivation for the Lennard-Jones potential sometimes seen in text books invokes the parameter, $\sigma$, thus:

$$r_{eqm,aa} = 2^{\frac{1}{6}} \sigma_{aa} \quad (12)$$

Lorentz-Berthelot combining rule is the most widely used to determine the unlike Lennard-Jones parameters. Lorentz [33] proposed to use the arithmetic mean for the unlike size parameter motivated by collisions of hard spheres using the following equation:

$$\sigma_{ab} = \frac{\sigma_{aa} + \sigma_{bb}}{2} \quad (13)$$

Berthelot [34] proposed with little physical argument for the geometric mean of the unlike energy parameter, leading to equation (14)

$$\varepsilon_{ab} = \sqrt{\varepsilon_{aa} \times \varepsilon_{bb}} \quad (14)$$

Then, the 12-6 Lennard-Jones potential becomes:

$$V_{12\text{-}6}(r) = 4\varepsilon_{ab}\left[\left(\frac{\sigma}{r}\right)^{12} - \left(\frac{\sigma}{r}\right)^{6}\right] \quad (15)$$

Thus, the coefficients $C_{12}$ and $C_6$ are given by:

$$C_{12} = \varepsilon_{ab} r_{eqm,ab}^{12} \quad (16)$$

$$C_6 = 2\varepsilon_{ab} r_{eqm,ab}^6 \quad (17)$$

General relationship between the coefficients ($C_6$, $C_{12}$), equilibrium separation ($V_{eqm}$), and well depth ($\varepsilon_{ab}$) are derived as follows. At the equilibrium separation, $r_{eqm}$, the potential energy is a minimum and equal to the well depth. The first derivative of the potential with respect to separation is zero at the minimum potential:

$$\left.\frac{dV}{dr}\right|_{V=V_{eqm}} = -\frac{nC_n}{r^{n+1}} + \frac{mC_m}{r^{m+1}} = 0 \quad (18)$$

Therefore,

$$\frac{nC_n}{r^{n+1}} = \frac{mC_m}{r^{m+1}} \quad (19)$$

$$C_m = \frac{nC_n r^{m+1}}{mr^{n+1}} = \frac{n}{m} C_n r^{(m-n)} \quad (20)$$

Substituting $C_m$ into equation (11) for $V(r)$, then at equilibrium:

$$-\varepsilon = \frac{C_n}{r_{eqm}^n} - \frac{nC_n r_{eqm}^{(m-n)}}{mr_{eqm}^m} \quad (21)$$

Equation (21) can be rewritten as:

$$-\varepsilon = C_n \left( \frac{mr_{eqm}^m - nr_{eqm}^n r_{eqm}^{(m-n)}}{mr_{eqm}^n r_{eqm}^m} \right) \quad (22)$$

The coefficient $C_n$ can be expressed in terms of m, n, $\varepsilon$ and $r_{eqm}$, as:

$$C_n = \frac{m}{n-m} \varepsilon r_{eqm}^n \quad (23)$$

By substituting into the original equation for $V(r)$:

$$C_m = \frac{n}{n-m} \varepsilon r_{eqm}^m \quad (24)$$

In summary, the general equation for any m and n will be:

$$V(r) \approx \frac{\frac{m}{n-m} \varepsilon r_{eqm}^n}{r^n} - \frac{\frac{n}{n-m} \varepsilon r_{eqm}^m}{r^m} \quad (25)$$

The examples of $r_{eqm}$ and $\varepsilon$ parameters used with AutoDock 4.0.1 for various atom types found in this study are listed in Table 2.2.

**Table 2.2** $r_{eqm}$ and $\varepsilon$ parameters for AutoDock 4.0.1 atom types [32].

| Atom type | $r_{eqm}$ (Å) | ε (kcal/mol) |
|---|---|---|
| H | 2.00 | 0.020 |
| C | 4.00 | 0.150 |
| N | 3.50 | 0.160 |
| O | 3.20 | 0.200 |
| F | 3.09 | 0.080 |
| Cl | 4.09 | 0.276 |
| Br | 4.33 | 0.389 |

***Grid maps*** [32]

AutoDock requires pre-calculated grid maps, one for each atom type presented in the guest being docked. These maps are calculated by AutoGrid. A grid map consists of a three dimension lattice of the regularly space points, surrounding and centered on some or all region of the host molecule. Typical grid point spacing varies from 0.2 to 1.0 Å although the default is 0.375 Å. Each point within the grid map stores the potential energy of a probe atom or functional group that is due to all the atoms in the host molecule.

Specific even number of grid points must be in each dimension, $n_x$, $n_y$ and $n_z$. This is because AutoGrid adds a central point, and AutoDock requires an odd number of grid points. The probe's energy at each grid point is determined by the set of parameters supplied for that particular atom type, and is the summation over all atoms of the host molecule, within a nonbonded cutoff radius, of all pairwise interactions. The following figure illustrates the main features of a grid map:

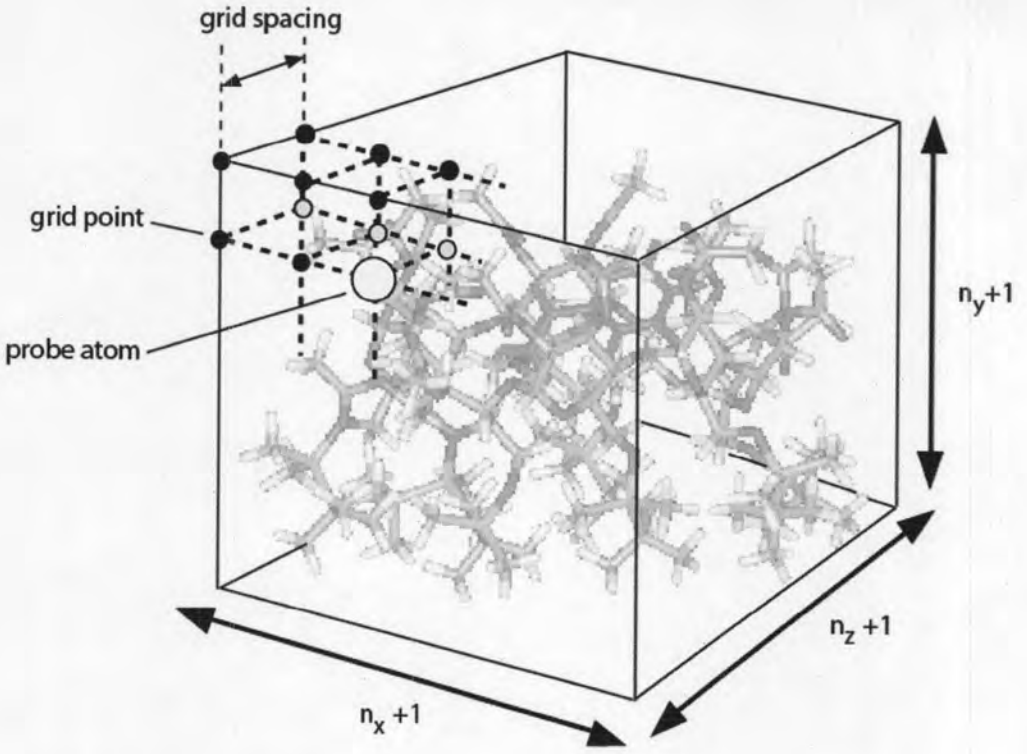


**Figure 2.3** The main feature of a grid map showing grid box dimensions ($n_x$, $n_y$, $n_z$= number of grid point in x-, y-, z- axis, respectively; C: gray; O: red; H; white; Si: yellow; guest molecule: green).

***Electrostatic potential grid maps*** [32]

In addition to the atomic affinity grid maps, AutoDock requires an electrostatic potential grid map. Polar hydrogens must be added, if the hydrogen bonds are being modeled explicitly. Partial atomic charges must be assigned to the host molecule. The electrostatic grid can be generated by AutoGrid. AutoGrid calculates Coulombic interactions between the host molecule and a probe with charge *e*; there is no distance cutoff used for electrostatic interactions. A sigmoidal distance-dependent dielectric function is used to model solvent screening, based on the work of Mehler and Solmajer [35],

$$\varepsilon(r) = A + \frac{B}{1 + ke^{-\lambda Br}} \qquad (25)$$

where $B = \varepsilon_0 - A$

$\varepsilon_0 = 78.4$ for the dielectric constant of bulk water at 25 °C

$A = -8.5525$

$\lambda = 0.003627$

$k = 7.7839$

$r$ = distance

Therefore, Coulombic interaction is derived according to equation (26)

$$V(\mathrm{r}) = \frac{q_i q_j}{4\pi\,\varepsilon(r) r_{ij}^2} \tag{26}$$

where $q_i$, $q_j$ = partial charge of atom i and j

### 2.6.2 Semi-empirical methods

Semi-empirical methods are simplified versions of Hartree-Fock theory using empirical corrections in order to improve performance. Within this construction, certain pieces of information, such as two-electron integrals, are approximated or completely omitted. In order to correct for the errors introduced by omitting part of the calculation, the method is parameterized. Parameters to estimate the omitted values are obtained by fitting the results to experimental data or ab initio calculations.

The most frequently used methods are Modified Neglect of Differential Diatomic Overlap (MNDO), Austin Model 1 (AM1), and Parametric Model number 3 (PM3). They are all based on the Neglect of Differential Diatomic Overlap (NDDO) integral approximation [36]. A number of additional approximations are made to speed up calculations and a number of parameterized corrections are made in order to correct for the approximate quantum mechanical model. How the parameterization is performed characterizes the particular semiempirical method. For the MNDO, AM1, and PM3, the parameterization is performed such that the calculated energies are expressed as heats of formations instead of total energies.

AM1, developed by Michael Dewar and co-workers in [37], is based on the NDDO integral approximation and is a generalization of MNDO approximation. It is an attempt to improve the MNDO model by reducing the repulsion of atoms at close separation distances. The atomic core-atomic core terms in the MNDO equations were

modified through the addition of off-center attractive and repulsive Gaussian functions.

PM3 is also based on the NDDO integral approximation. It was developed by J. J. P. Stewart [38] and uses the same formalism and equations as the AM1 method. The only two differences are PM3 uses two Gaussian functions for the core repulsion function, instead of the variable number used by AM1, and the numerical values of the parameters are different.

Semi-empirical calculations have been very successful in the description of organic chemistry, where there are only a few elements used extensively and the molecules are moderate size. In 2000, Li and co-workers [39] performed some studies about the performances of AM1 and PM3 methods on CD systems. They suggested that PM3 should be advantageous to AM1 in CD chemistry because PM3 can deal with the O–H···O hydrogen bonds better than AM1. This study was supported by direct structure optimization of α- and β-CD with AM1 and PM3, in which AM1 gave badly distorted geometries due to unreasonable hydrogen bonding, whereas PM3 reproduced the crystalline structures rather well. Therefore, PM3 calculation was chosen to optimize the host structure and energy calculations in this study.